Two-photon resonance assisted huge nonlinear refraction and absorption in ZnO thin films

Ja-Hon Lin, Yin-Jen Chen, Hung-Yu Lin, and Wen-Feng Hsieh

Citation: Journal of Applied Physics **97**, 033526 (2005); doi: 10.1063/1.1848192
View online: http://dx.doi.org/10.1063/1.1848192
View Table of Contents: http://scitation.aip.org/content/aip/journal/jap/97/3?ver=pdfcov
Published by the AIP Publishing

Two-photon resonance assisted huge nonlinear refraction and absorption in ZnO thin films

Ja-Hon Lin, Yin-Jen Chen, Hung-Yu Lin, and Wen-Feng Hsieh[a)]
Institute of Electro-Optical Engineering, National Chiao-Tung University, 1001, Ta-Hsueh Rd., Hsinchu 300, Taiwan

(Received 16 September 2004; accepted 16 November 2004; published online 19 January 2005)

Optical nonlinearities of ZnO thin films, made by laser deposition, were investigated by the *Z*-scan method using a mode-locked femtosecond Ti:sapphire laser. The measured bound-electron nonlinear index of refraction γ and the two-photon absorption coefficient β at near-IR wavelengths show an enormous enhancement compared with measurements on bulk ZnO at 532 nm. The results reveal that two-photon resonance to the band edge and exciton energy level is responsible for the nonlinear absorption and that the free carrier induced the optical nonlinearity. With the excitation wavelength operated between 810 to 840 nm, a negative β value is measured due to the saturation of linear absorption of the defect states. Finally, we compared the values of β from the closed aperture *Z*-scan data (by considering the multi-photon absorption induced thermal nonlinearity) with those obtained from the open aperture *Z*-scan data. The results show that nonlinear refraction in the near-IR region is dominated by the bound-electron and free-carrier effect, although the thermal optical nonlinearity cannot be completely ignored. © *2005 American Institute of Physics*. [DOI: 10.1063/1.1848192]

I. INTRODUCTION

It has been of great interest that wide-gap semiconductors such as GaN and ZnO can be developed into blue-green laser diodes and photonic devices. ZnO has a band gap of 3.37 eV (wavelength ~368 nm) at room temperature and a large exciton binding energy with high excitonic gain. Therefore, it can be a good candidate for ultraviolet photonic device applications.[1–3] Recently, room-temperature optically pumped ultraviolet laser emission has been observed in ZnO thin films that were attributed to exciton–exciton scattering and electron–hole plasma recombination processes.[4] Besides the applications of ZnO in ultraviolet photonic devices, the nonlinear properties of ZnO are also attractive.[5–10] It has been pointed out that ZnO thin films have large nonlinear second-order optical susceptibility $\chi^{(2)}$, which results in efficient second-harmonic generation (SHG).[5,6] A systematic study of SHG as a function of ZnO film thickness[6] shows that the value of $\chi^{(2)}$ for very thick films is larger than that of the bulk single-crystal ZnO. Very high conversion efficiency of the third-harmonic radiation[7] is also achieved by using an unamplified femtosecond Cr^{4+}:forsterite laser as the excitation source on a submicron-thin nanocrystalline ZnO film that was pulsed-laser deposited on a fused silica substrate.

Furthermore, the bound-electron nonlinear refractive index γ, two-photon absorption (TPA), and the free-carrier-induced nonlinear absorption σ_r, which represents the refractive index change per carrier-pair density, have been measured in the bulk ZnO crystal with the excitation photon energy well below the absorption band edge.[8,9] With the use of a single-beam *Z*-scan technique under nonresonant condition, $\beta = 4.2 \pm 0.9$ cm/GW, $\gamma = -(0.9 \pm 0.3) \times 10^{-14}$ cm^2/W, and $\sigma_r = -(1.1 \pm 0.3) \times 10^{-21}$ cm^3 were measured in 1 mm ZnO single crystal by 25 ps pulses of a 532 nm green laser.[8,9] From cryogenic temperature to room temperature, the third-order optical nonlinearity ($\chi^{(3)}$) of ZnO microcrystallite thin films near exciton resonance has also been reported to be between 10^{-7} and 10^{-4} esu, using the femtosecond time-resolved degenerate four-wave mixing (DFWM) method.[10]

In this article, we experimentally investigated the optical nonlinear property of ZnO microcrystalline thin films, by using the single-beam *Z*-scan technique near two-photon resonance at both the band edge and exciton energy level, under illumination of a femtosecond Ti:sapphire laser. Our c-axis-oriented 1-μm-thick ZnO thin film was grown on a quartz substrate by high-vacuum laser deposition at 600 °C and *in situ* postannealed at 700 °C for 1 h. The experimental setups for various measurements are described in the next section. In Sec. III, the fundamental optical property of the ZnO thin film and the results of the *Z*-scan measurement are revealed. Further analysis of the results is carried out by taking the thermal-optical nonlinear refraction into account. Finally, conclusions are drawn in Sec. IV.

II. EXPERIMENT

A UV 325 nm He-Cd laser (Kimmon IK5552R-F) was utilized as a pumping source for photoluminescence (PL) measurement. The PL emission was dispersed by a single-grating monochromator (TRIAX 320) and then detected by a photomultiplier tube (PMT-HVPS) that was equipped with a photon counter. The spectral reflectance was measured by the VW configuration of the experimental setup using a Lambda 900 spectrometer (PerkinElmer Inc.). The sample was properly rotated with a small angle and excited by the continuous white light, and then the reflectance from the interface of the sample was collected on the detector. Similarly, the transmittance of the sample was measured by detecting the transmit-

a)Author to whom the correspondence should be addressed; electronic mail: wfhsieh@mail.nctu.edu.tw

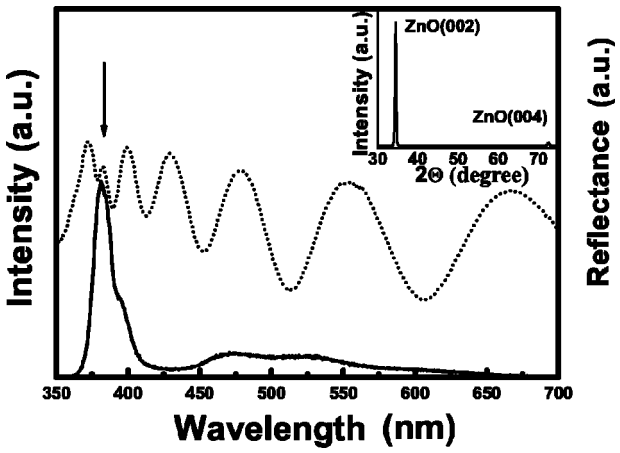

FIG. 1. Spectra of PL (solid curve) and reflectance (dotted curve) of the ZnO thin film with the arrow showing the exciton peak at 380 nm. The inset is the x-ray diffraction pattern.

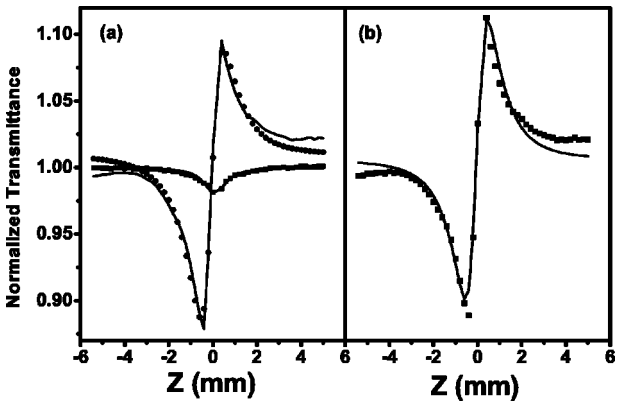

FIG. 2. The *Z*-scan traces for (a) the open aperture ($S=1$, solid squares) and the closed aperture ($S=0.4$, solid circles), and (b) the result of dividing the $S=0.4$ value by the $S=1$ value by exciting the laser with $I_0=2.05$ GW/cm^2 at 745 nm. The solid curve is the fitting result from the theory.

ted light passing through the sample. The absorption coefficient was then calculated from the transmittance and the reflectance. A standard degenerate *Z*-scan measurement[11–14] was performed by using as a pump source a commercial femtosecond Ti:sapphire laser (Coherent Mira-900F) with 76 MHz repetition rate (f) and 175 fs pulse width (t_0). The output of the exciting laser was chopped and then divided into two beams by a beam splitter with one as the excitation light that was focused on the sample by a 5 cm focal-length lens. The sample was mounted on a step-motor in order to precisely move along the *Z* axis. The transmitted light through the sample and an aperture was detected by a photodiode as the signal. The other beam, which acted as the reference, was detected by another photodiode for monitoring the output fluctuation of the pumping laser. Both outputs of the two photodiodes were simultaneously connected to a lock-in amplifier (Stanford research SR830) for improving the signal-to-noise ratio. The normalized transmittance was obtained through a simple division of the acquired sample signal by the reference signal. In our measurement, we opened the aperture completely to detect the *Z*-dependent normalized transmittance ($S=1$ *Z*-scan trace) and then closed the aperture to obtain the $S=0.4$ *Z*-scan trace.

III. RESULTS AND DISCUSSION

The room-temperature PL spectrum of the ZnO thin film (solid curve in Fig. 1) shows a near-band-edge emission around 380 nm and a weak broadband emission around 450–550 nm that is attributed to the deep-level emission related to the Zn vacancy or excess oxygen.[15,16] The spectral reflectance (dotted curve in Fig. 1) reveals interference fringes accompanied with an extra peak at 380 nm that corresponds to the exciton resonance, as the PL spectral peak. From the interference fringes we estimated the film thickness is about 1 μm, which is consistent with that measured by the surface profile measurement. Furthermore, from the transmittance (not shown here) and reflectance spectra, we also calculated the linear absorption coefficient $\alpha=705$ cm^{-1} for wavelength of 745 nm. In the inset of Fig. 1, strong x-ray diffraction lines from the (002) and (004) planes reveal that the *c* axis of ZnO film is parallel to the growth direction or the normal to the substrate.

The *Z*-scan traces of open aperture $S=1$ (solid squares) and closed aperture $S=0.4$ (solid circles), measured at a wavelength of 745 nm with pump irradiance $I_0=2.05$ GW/cm^2, are shown in Fig. 2. In contrast with the negative nonlinear refraction measured at a wavelength of 532 nm,[8,9] the valley-peak configuration of the $S=0.4$ *Z*-scan trace in Fig. 2(a) indicates that our ZnO thin film has a positive nonlinear refraction at near-IR wavelengths. By curve fitting of the $S=1$ *Z*-scan trace with the traditional *Z*-scan theory,[11] we obtained $\beta=278$ cm/GW from the solid curve of Fig. 2(a). A symmetric *Z*-scan trace (solid squares) in Fig. 2(b) was obtained from the division of the $S=0.4$ *Z*-scan data by the $S=1$ data of Fig. 2(a) to eliminate the nonlinear absorption. Then, the fitting parameters including phase distortion $\Delta\Phi$ and Rayleigh range z_0 can be determined from the fitted solid curve[11–14] in Fig. 2(b). Using the relation $\Delta\Phi=(2\pi/\lambda)\Delta n L_{\text{eff}}$,[14] the nonlinear refractive index Δn can be calculated if the wavelength λ of incident laser and the $L_{\text{eff}}=(1-e^{-\alpha L})/\alpha$ are known, where α is the absorption coefficient and L is the thickness of the measured sample. From the measured $L=1$ μm and $\alpha=705$ cm^{-1}, we calculated $L_{\text{eff}}\sim 980$ nm and deduced the third-order nonlinear index of refraction to be $\gamma=+3.125\times10^{-11}$ W/cm^2 from $\Delta n=\gamma I_0$. The positive sign of γ is consistent with the theoretical prediction based on the two-parabolic-band (TPB) model and the Kramers–Kronig (K-K) relation.[13]

The best-fit results of β (hollow circles) and $\Delta n/I_0$ (solid squares) from the *Z*-scan measurements as a function of the incident peak irradiance at 745 nm are shown in Fig. 3. Similar with the previous reports,[8,9] in which the nonlinear absorption is dominated by TPA, our measured value of β is irradiance independent and has on average a value of 297 cm/GW marked by the dashed line in Fig. 3. If one considers the influence of β on L_{eff}, then L_{eff} can be expressed as $L_{n,\text{eff}}=(1-e^{-(\alpha+\beta_2 I)L})/(\alpha+\beta_2 I)$. Using the parameters $\beta=297$ cm/GW and $I_0=1.6$ GW/cm^2, we obtained

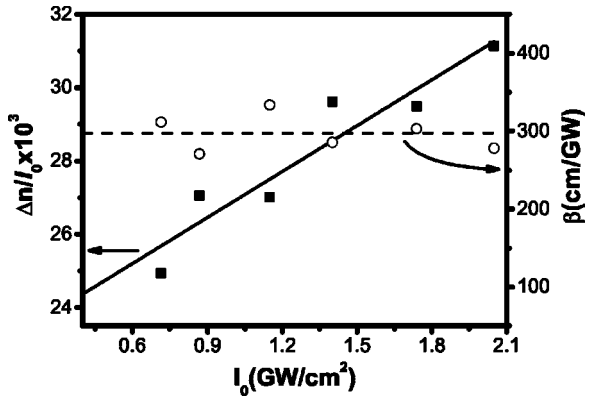

FIG. 3. The measured $\Delta n/I_0$ (solid squares) and β (hollow circles) of the ZnO thin film as a function of excitation irradiance for exciting at 745 nm.

$L_{n,\mathrm{eff}} \sim 930$ nm. Therefore, the nonlinear absorption causes a negligible change of L_{eff} of only 5%.

At high irradiance, the nonlinear refractive index Δn versus the irradiance is no longer linear due to the influence of free carriers generated by TPA.[12] By fitting the relation[12]

$$\Delta n/I_0 \cong \gamma + C\sigma_r I_0 \tag{1}$$

to the experimental data as the solid curve in Fig. 3, we obtained $\gamma = +(2.26 \pm 0.11) \times 10^{-11}$ cm^2/W or $+(1.068 \pm 0.047) \times 10^{-8}$ esu that is three orders of magnitude larger than that obtained for the single-crystal ZnO bulk with $\gamma = -(0.9 \pm 0.3) \times 10^{-14}$ cm^2/W when excited by the green laser at 532 nm.[8,9] Note that the listed errors here are the fitting errors, which do not consider the systematic errors such as the measurement errors of the beam waist, pulse width, and average power of the laser. The enormous increase of nonlinearity in the thin film in comparison with that in the bulk had been widely reported previously. For example, the enhancement of the second-order susceptibility $\chi^{(2)}$ in the ZnO microcrystalline thin film is reported due to the stacking quality.[6] In use of the femtosecond DFWM technique,[10] the third-order susceptibility $\chi^{(3)}$ of the ZnO microcrystalline thin film had been reported to range from 10^{-7} to 10^{-4} esu when it was excited near the excitonic resonance. For low linear absorption ($\alpha_0 L < 0.2$), the parameter $C \cong 0.23(\beta t_0/\hbar\omega)$ of Eq. (1) can be obtained from the pulse width t_0 of the excitation source and the TPA coefficient β. Therefore, we estimate that the value of σ_r is 9.28×10^{-20} cm^3, in which the positive sign is opposite to the reported negative values for bulk results.[8,9]

We summarized the values of β (squares) and σ_r (circles) versus the excitation wavelength in Fig. 4(a). At the low photon energy (longer excitation wavelength) end, both β and σ_r are quite small, but they start to increase at around 766 and 770 nm, respectively. β reaches its first maximum at 760 nm and then slightly falls and rises again at around 745 nm. Finally, it maintains almost constant toward the shorter excitation wavelength. As previously mentioned, the exciton peak at 380 nm is indicated in the PL and reflectance spectra of Fig. 1. The first maximum of β at 760 nm corresponds to two-photon resonance to the exciton level and the second take-off wavelength at 745 nm corresponds to a half of the bandgap energy ($E_g = 3.328$ eV). Note that the difference of

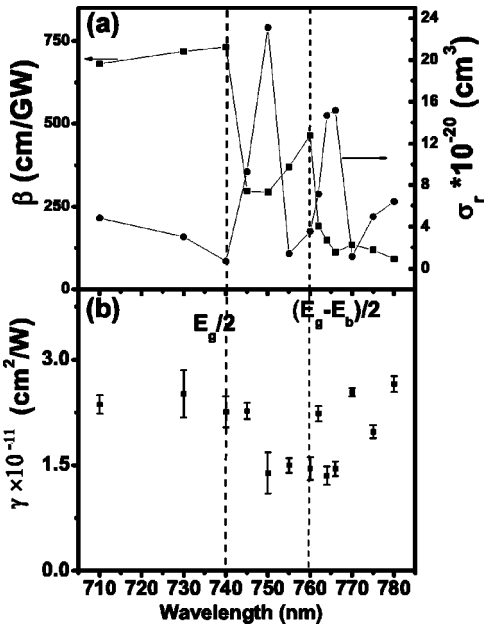

FIG. 4. The near-IR spectral responses of β (solid squares) and σ_r (solid circle) (a), and γ (solid squares with small error bar) (b).

photon energies between 745 and 760 nm equals nearly one-half of the binding energy of free exciton (around 60 meV). Therefore, the spectral response of β reflects TPA near resonance to the exciton energy level and the band edge of ZnO film. The maximum value of $\beta = 732$ cm/GW at 740 nm shows an enhancement of 174 times than $\beta = 4.2$ cm/GW obtained for the ZnO bulk crystal.[8,9] Exciton enhancement of the TPA was reported in GaAs quantum well when the exciton energy was twice the incoming photon energy.[17,18] The exciton-assisted enhancement of nonlinear absorption in GaN thin films with 100 times larger than off-resonance values was also reported using femtosecond pump-probe techniques.[19]

The spectral response of σ_r (solid circles) in Fig. 4(a) also reveals two peaks at 766 and 750 nm, which were slightly redshifted relative to the exciton energy level and the band edge of ZnO film. Nevertheless, the difference between two spectral peaks of σ_r still satisfies one-half of the exciton binding energy. This shift may be due to too many carriers being generated to cause band-filling, or due to a less effective pump excitation volume of TPA for large values of β.[8,9] However, the wavelength dependence of nonlinear refraction γ in Fig. 4(b) shows no apparent tendency but is alternating within a small range. This results from the too small tuning range of our excitation wavelength, which could not reveal a significant change of γ as predicted by the TPB model and the K-K relation.[13] The values of measured nonlinear parameters, including γ, β, and σ_r near-IR wavelengths, are revealed in Table I.

When the excitation laser wavelengths were set between 810 and 840 nm, a symmetric peak instead of a deep of $S = 1$ Z-scan trace can be seen. The solid circles in Fig. 5(a) reveal the measured $S = 1$ Z-scan trace excited at 830 nm with an irradiance of 1.86 GW/cm^2. This behavior has been experimentally reported previously due to saturation of the linear absorption.[20,21] The effectively negative TPA coefficient,

TABLE I. The measured nonlinear parameters including the $\gamma, \beta, \sigma_r, q, \beta_{\text{th}}$, and β/β_{th} for the excitation wavelength near IR.

λ (nm)	$\gamma\times10^{-11}$ (cm^2/W)	β (cm/GW)	$\sigma_r\times10^{-20}$ (cm^3)	q	β_{th} (cm/GW)	β_{th}/β
710	2.36	681	4.83	2.00	30391	44.6
730	2.51	718	3.02	2.02	22444	31.3
740	2.26	732	0.71	1.98	15505	21.2
745	2.27	297	9.28	2.02	21529	72.5
750	1.39	292	23.11	1.85	16637	57.0
755	1.50	370	1.41	2.15	16277	44.0
760	1.45	464	3.56	2.20	18403	39.7
762	2.23	191	7.14	1.91	18116	94.8
764	1.35	148	14.68	2.06	13615	92.0
766	1.45	112	15.15	2.09	16226	144.9
770	2.54	134	1.14	2.01	17821	133.0
775	1.98	116	4.98	2.17	19859	171.2
780	2.65	91	6.42	2.03	19384	213.0

obtained by the fitting to the experimental data (shown as solid curve in Fig. 5), was −153.13 cm/GW and resulted from the saturation of the ZnO defect state. In contrast, the valley-peak $S=0.4$ *Z*-scan trace [solid squares in Fig. 5(a)] and the symmetric normalized transmittance obtained by the dividing result [Fig. 5(b)] show a positive nonlinear refraction of $\gamma=+2.56\times10^{-11}$ cm^2/W.

As predicted by the TPB,[13] the nonlinear refraction of semiconductor materials will become negative when the excitation photon energy is tuned above $0.7E_g$, as experimentally demonstrated by the negative γ value obtained for ZnO single crystal using the exciting picosecond *Q*-switched laser at 532 nm.[8,9] We therefore used the 420 nm UV pumping source from the frequency-doubled femtosecond mode-locked Ti:sapphire laser for the *Z*-scan measurement. We observed large transmittance in $S=1$ (solid squares) and $S=0.4$ (solid circles) *Z*-scan traces, shown in Fig. 6(a), which reveal enormous TPA. The positive Δn can be seen after dividing the result of $S=0.4$ by the $S=1$ one in Fig. 6(b). The positive γ under excitation wavelength of 420 nm seems to be violating the dispersion relation of γ predicted by TPB.[13] We therefore suspected that the nonlinear refraction may come mainly from the thermal-optical effect due to continuous illumination of the high repetition rate pulses. Thermal

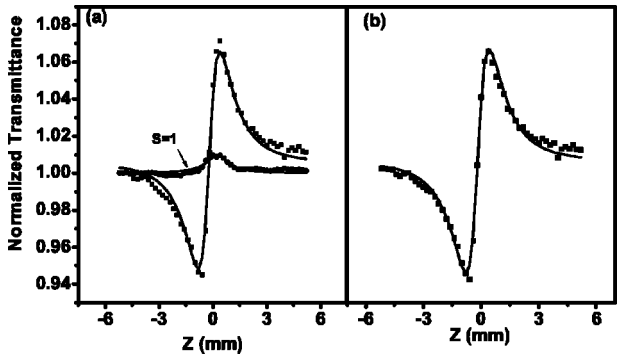

FIG. 5. The *Z*-scan traces at 830 nm with $I_0=1.86$ GW/cm^2 of the open aperture ($S=1$, solid squares) and closed aperture ($S=0.4$, solid circles) (a), and the result of dividing $S=0.4$ by $S=1$ values (b). The solid curve is the theoretically fitting result.

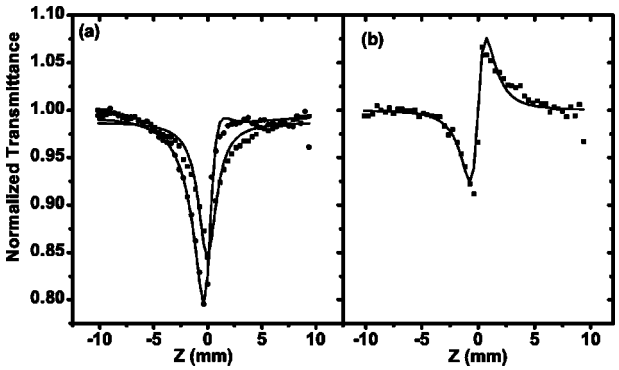

FIG. 6. The *Z*-scan traces for (a) the open aperture (solid squares) and the closed aperture (solid circles), and (b) the result of dividing $S=0.4$ by $S=1$ values shows the positive refraction for 420 nm with $I_0=0.35$ GW/cm^2. The solid curve is the theoretically fitting result.

optical nonlinearity will occur if the thermal characteristic time $t_c=\omega_0^2\rho c_p/4\kappa$ is longer than the repeat period of laser pulses. Using the parameters of beam radius ω_0 around 11 μm, density $\rho=5.67$ g/cm^3, specific heat $c_p=9.6$ $\text{cal mol}^{-1}\,\text{K}^{-1}$, and thermal conductivity $\kappa=0.54$ $\text{W cm}^{-1}\,\text{K}^{-1}$ of ZnO,[22] we estimated $t_c\sim1.6$ μs, which is much longer than the period of laser pulses about 13 ns. Therefore, the thermal-optical nonlinearity may not be eliminated in our closed-aperture *Z*-scan measurement.

Let us assume that the normalized transmittance alternation in a closed-aperture *Z*-scan trace is completely due to the index change Δn from the thermal-optical nonlinearity by *q*-photon absorption. The time-dependent normalized transmittance can then be expressed as[23]

$$\frac{I(\xi,t)}{I(0,0)}=1+\frac{\vartheta(q)}{q}\frac{1}{(1+\xi^2)^{q-1}}\tan^{-1}\times\left(\frac{2q\xi}{[(2q+1)^2+\xi^2]\frac{t_c(\xi)}{2qt}+2q+1+\xi^2}\right), \tag{2}$$

and

$$\vartheta(q)=kL\frac{qh\upsilon H(q)N\sigma_q f}{2\pi\kappa}\frac{dn}{dT}\left(\frac{2}{\pi\omega_0^2}\right)^{q-1}, \tag{3}$$

$$\text{with } H(q)=\int p^q(t)dt, \tag{4}$$

where $p(t)$ (in s^{-1}) is proportional to the instantaneous power of the pulse and the integration is over the pulse duration; N is the density of the absorbing centers (cm^{-3}); ω_0 is the spot size of the laser at the focus; f is the repetition rate of the laser; σ_q is the multiphoton absorption cross section ($\text{cm}^{2q}\,\text{s}^{q-1}$); $k=2\pi/\lambda$, with λ being the central wavelength of the exciting light; $\xi=z/z_0$; and $dn/dT=0.7\times10^{-4}\,\text{k}^{-1}$ is thermal-optical coefficient of ZnO crystal. As reported,[23] ΔT_{p-v} approaches a constant value while $t/t_c>10$. The time-dependent normalized transmittance of Eq. (1) can then be reduced to the time-independent relation

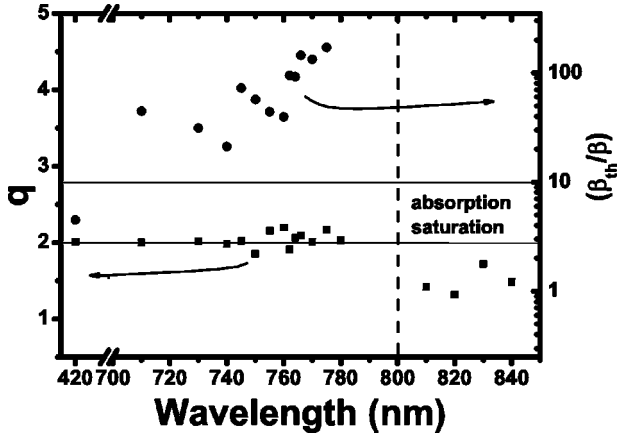

FIG. 7. β_{th}/β and q versus the different excitation wavelengths.

$$\frac{I(\xi)}{I(0,0)} = 1 + \frac{\vartheta(q)}{q}\frac{1}{(1+\xi^2)^{q-1}}\tan^{-1}\left(\frac{2q\xi}{2q+1+\xi^2}\right). \qquad (5)$$

By fitting the measured data of Fig. 6(b) to Eq. (5), we obtain the fitting parameters $q=2.07$ and $\vartheta(q)=0.51$. At the value of q around 2, the TPA-induced thermal nonlinearity is dominant, as the sample is excited just below the band gap; e.g., at 420 nm. Using $q=2$ and $\vartheta(q)=0.51$ and calculating $H(q)$ from given $p(t)$, we obtained $N\sigma_q$ according to Eq. (3). By the relation $\beta_{th}=2N\sigma_q/h\nu$, we further estimated $\beta_{th}=2.16\times10^5$ cm/GW for completely TPA-induced thermal heating. It is close to the measured value of $\beta=4.79\times10^4$ cm/GW obtained from the $S=1$ *Z*-scan result of Fig. 6(a) [within an order of magnitude $(\beta_{th}/\beta\sim5)$]. The result suggests that the thermal-optical nonlinearity is the major influence in the UV region and the overestimation may come from the inaccuracy of the parameters of bulk ZnO used for determining β_{th}.

In order to investigate the thermal optical nonlinearity in the near-IR region, we fitted the normalized *Z*-scan trace to Eq. (5) and obtained q (solid squares) and β_{th}/β (solid circles) versus the excitation wavelength in Fig. 7. While the excitation wavelengths are below 780 nm, the fitted values of q around 2 reveals TPA occurrence around the two-photon resonance at the band edge. Nevertheless, the q value below 2, obtained while the excitation wavelength was set between 810 and 840 nm, reflects the saturation of linear absorption of the ZnO defect states within this range. It is worthwhile to notice that the measured β and the estimated β_{th} is much larger in the blue range than in the near-IR range due to near-single one-photon resonance at the band edge; hence large heat deposition causes apparent distortion of the wave front. In addition, the estimated β_{th} is close to the measured β only when the excitation wavelength is around 420 nm with the ratio $\beta_{th}/\beta\sim5$ from Fig. 7. Thus, the positive nonlinear refraction around 420 nm violates the expected negative β that may be due mainly to the thermal-optical effect. Contrarily, the estimated β_{th} is far larger than the measured β in the near-IR with the ratio $\beta_{th}/\beta>10$ to show the minor influence of heat at this excitation wavelength range. Notice that there are two dips in the plot of β_{th}/β (Fig. 7) at the excitation wavelengths of 745 and 760 nm, which correspond to two-photon resonance at the band edge and the free exciton energy level. The decrease of β_{th}/β is due to an increase of the measured β with no apparent change of β_{th}, which indicates the increasing influence of the thermal-optical effect. The calculated values of q, β_{th}, and β_{th}/β are also summarized in Table I for comparison. According to the TPB model based on the K-K relation,[13] it shows a significant resonant feature but rather smooth spectral response of nonlinear refraction near the two-photon resonances. Thus, the nonlinear refraction is induced mainly by bound-electronic and free-carrier effects for near-IR excitation between 710 and 780 nm. Nevertheless, it still shows great thermal perturbation causing fluctuation of γ as shown in Fig. 4(b). However, the nonlinear refraction is dominated by the thermal-optical nonlinearity, when the excitation photon energy is chosen above $0.7E_g$, e.g., for excitation wavelength <420 nm.

IV. CONCULSION

Optical nonlinearities of ZnO thin film deposited by pulsed laser have been investigated by the *Z*-scan method using the high repetition rate femtosecond Ti:sapphire laser tuned from 710 to 840 nm as well as at frequency-doubled wavelengths. This is a *Z*-scan measurement of ZnO thin films near one-half band edge. We measured an enormous enhancement of γ and β as compared with that obtained in bulk ZnO, measured at 532 nm with 25 ps pulse duration. In addition, the two-photon near resonance to the band edge and free exciton energy level can be seen from the β and σ_r. Nevertheless, the redshift of two peaks in σ_r relative to the β might be due to the free carrier saturation. By tuning the excitation wavelength within 810–840 nm, an effective negative two-photon absorption coefficient is measured due to saturation of the linear absorption of the ZnO defect states. The ratio of the β_{th}/β suggests that bound electrons and free carriers are the main causes of the nonlinear refraction for the excitation wavelength at near-IR, although the thermal optical nonlinearity cannot be completely eliminated. However, thermal-optical nonlinearity is dominating in cases in which the exciting wavelengths are shorter than 420 nm. The occurrence of a two-photon absorption process is revealed for q values around 2 within the range from 710 to 780 nm. A q value below 2 at an excitation wavelength between 810 to 840 nm results from one-photon absorption of the ZnO defect states.

ACKNOWLEDGMENT

This work is partially supported by the National Science Council (NSC) of Taiwan under grant NSC 93-2811-M-009-032. One author (J.-H. L.) would like to thank NSC for providing postdoctor fellowship, and another (S.-Y. K.) in Precision Instrument Development Center for experimental help.

[1] D. M. Bagnal, Y. F. Chen, Z. Zhu, T. Yao, S. Koyama, M. Y. Shen, and T. Goto, Appl. Phys. Lett. **70**, 2230 (1997).
[2] Z. K. Tang, G. K. L. Wong, P. Yu, M. Kawasaki, A. Ohtomo, H. Koinuma, and Y. Segawa, Appl. Phys. Lett. **72**, 3270 (1998).
[3] H. Cao, Y. G. Zhao, S. T. Ho, E. W. Seelig, Q. H. Wang, and R. P. H. Chang, Phys. Rev. Lett. **82**, 2278 (1999).
[4] D. M. Bagnall, Y. F. Chen, Z. Zhu, T. Yao, M. Y. Shen, and T. Goto, Appl. Phys. Lett. **73**, 1038 (1998).

[5]H. Cao, J. Y. Wu, H. C. Ong, J. Y. Dai, and R. P. H. Change, Appl. Phys. Lett. **73**, 572 (1998).
[6]G. Wang, G. T. Kiehne, G. K. L. Wong, J. B. Ketterson, X. Liu, and R. P. H. Chang, Appl. Phys. Lett. **80**, 401 (2002).
[7]G. I. Petrov, V. Shcheslavskiy, V. V. Yakovlev, I. Ozerov, E. Chelnokov, and W. Marine, Appl. Phys. Lett. **83**, 3993 (2003).
[8]X. J. Zhang, W. Ji, and S. H. Tang, J. Opt. Soc. Am. B **14**, 1951 (1997).
[9]X. Zhang, H. Fang, S. Tang, and W. Ji, Appl. Phys. B: Lasers Opt. **65**, 549 (1997).
[10]W. Zhang, H. Wang, K. S. Wong, Z. K. Tang, and G. K. L. Wong, Appl. Phys. Lett. **75**, 3321 (1999).
[11]M. Sheik-Bahae, A. A. Said, T. H. Wei, D. J. Hagan, and E. W. Van Stryland, IEEE J. Quantum Electron. **26**, 760 (1990).
[12]A. A. Said, M. Sheik-Bahae, D. J. Hagan, T. H. Wei, J. Wang, J. Young, and E. W. Van Stryland, J. Opt. Soc. Am. B **9**, 405 (1992).
[13]M. Sheik-Bahae, J. Wang, and E. W. Van Stryland, IEEE J. Quantum Electron. **30**, 249 (1994).
[14]Y. C. Ker, J. H. Lin, and W. F. Hsieh, Jpn. J. Appl. Phys., Part 1 **42**, 1258 (2003).
[15]K. Vanheusden, C. H. Seager, W. L. Warren, D. R. Tallant, and J. A. Voigt, Appl. Phys. Lett. **68**, 403 (1996).
[16]B. Lin, Z. Fu, and Y. Jia, Appl. Phys. Lett. **79**, 943 (2001).
[17]A. Obeidat and J. Khurgin, J. Opt. Soc. Am. B **12**, 1222 (1995).
[18]C. C. Yang, A. Villeneuve, G. I. Stegeman, C.-H. Lin, and H.-H. Lin, IEEE J. Quantum Electron. **29**, 2934 (1993).
[19]K. H. Lin, G. W. Chern, Y. C. Huang, S. Keller, S. P. DenBaars, and C. K. Sun, Appl. Phys. Lett. **83**, 3087 (2003).
[20]Y. L. Huang, C. K. Sung, J. C. Liang, S. Keller, M. P. Mack, U. K. Mishra, and S. P. DenBaars, Appl. Phys. Lett. **75**, 3524 (1999).
[21]J. He, W. Ji, G. H. Ma, S. H. Tang, H. I. Elim, W. X. Sun, Z. H. Zhang, and W. S. Chin, J. Appl. Phys. **95**, 6381 (2004).
[22]R. Bhargava, *Properties of Wide Bandgap II-VI Semiconductors* (The Institution of Electrical Engineers, London, 1997), p. 28.
[23]M. Falconieri, J. Opt. A, Pure Appl. Opt. **1**, 662 (1999).